DALTON

Deposition and growth of noble metal clusters on graphite *

Gareth M. Francis, Ian M. Goldby, Laurens Kuipers, Bernd von Issendorff and Richard E. Palmer

Nanoscale Physics Research Laboratory, School of Physics and Space Research, University of Birmingham, Edgbaston, Birmingham B15 2TT, UK

The growth of silver and gold clusters following atomic vapour deposition on highly oriented pyrolytic graphite has been studied using scanning electron microscopy and scanning tunnelling microscopy (STM). Three-dimensional clusters were grown on the terraces and quasi-one-dimensional chains of clusters along the surface steps. An STM study was made on the effect of the step height on cluster nucleation. Charge-density modulations on the substrate surface around the silver clusters were analysed. A preliminary study of the deposition of mass-selected silver clusters from a beam onto the graphite surface has been made. The effect of the impact energy of silver clusters on the deposition process is explored.

Metal clusters can be regarded as nanometer-scale building blocks for the construction of novel materials.[1] Such applications require the deposition of clusters on a substrate. Moreover, the possibility of incorporating metal clusters into nanometer-scale electronic (or photonic) devices[2] requires not only the deposition but also the organisation of clusters on a surface. These are the issues which we explore in this paper, *via* two complementary approaches: (*i*) nucleation of clusters from deposited atoms at selected surface sites, and (*ii*) deposition of size-selected clusters from a cluster beam.

Several studies of the deposition of metal atoms on highly oriented pyrolytic graphite substrates have been reported recently. These have mainly dealt with the simultaneous growth of two- and three-dimensional atomic clusters on the substrate. In a previous study we investigated the growth mechanism of silver clusters on surface terraces and steps,[3] and were able to grow three-dimensional clusters on the terraces and to produce quasi-one-dimensional cluster chains along the steps. By control of the substrate temperature and the deposition rate we were able to favour the growth at steps and suppress terrace nucleation.

Scanning tunnelling microscopy (STM) has been extensively used to study the growth of transition and noble metals on graphite. Ganz *et al.*[4] have studied two-dimensional islands of Ag and Au and found them to be weakly bonded to, and incommensurate with, the substrate. Other groups have studied three-dimensional clusters of Pt,[5,6] Pd[7] and Mo[8] on graphite and periodic charge-density modulations (CDMs) have been occasionally seen around these clusters. Similar modulations have also been seen near defects on the surface, like holes[9] and steps.[10] It has generally been agreed that these charge-density modulations, which have a periodicity of $(\sqrt{3} \times \sqrt{3})$ rotated by 30° with respect to the underlying graphite lattice, are not caused by physical surface-atom rearrangements. Indeed, they have many different structures. Xhie *et al.*[5] have catalogued ten different structures and Mizes and Foster[11] have suggested that these CDMs are due to interference between the surface electron wavefunctions and scattered waves from the defect or cluster. They calculated STM images using a tight-binding model but could not reproduce the experimentally observed structures. Simulations of the CDMs have been produced,[6] which do not treat scattering by the cluster/defect, but simply consider the interference of multiple electron wavefunctions, corresponding to the Fermi wave vector, with arbitrary magnitude and phase. These simulated modulations compare well to those seen experimentally.

Less attention has been paid to the growth of clusters at the natural surface steps on graphite. Platinum, palladium and copper clusters have been seen by either transmission electron microscopy or STM to decorate steps.[12–14] In our previous scanning electron microscopy (SEM) study of the growth of silver clusters on terraces and at steps[3] we found evidence that large clusters were mobile along the steps and on the terraces. This resulted in the aggregation of clusters into larger islands. We also found evidence for different types of steps on the surface, as indicated by the amount of cluster nucleation that took place at the different steps.

In this work we provide further evidence, obtained with STM, that the height of a step is an important factor in determining the amount of nucleation (of silver and gold clusters) that occurs at a step edge on the graphite (0001) surface. We also analysed two- and three-dimensional clusters of Ag on the terraces, showing that only larger three-dimensional clusters cause charge-density modulations, except when two-dimensional clusters are nucleated at a defect on the substrate. This STM study of clusters produced by nucleation of deposited atoms is complemented by our first SEM images of silver clusters deposited from a mass-selected cluster source. We found evidence for cluster implantation, cluster diffusion and cluster decoration of the surface steps, depending on the deposition conditions.

Experimental

Atomic vapour deposition

Highly oriented pyrolytic graphite (HOPG) substrates were cleaved in air and placed immediately in a vacuum chamber. Deposition was carried out in high vacuum with a base pressure of 10^{-6} Torr. Silver (purity >99.99%) or Au (purity 99.999%) was evaporated from a graphite crucible through a nozzle of 1 mm diameter. The substrates were situated 24 cm from the nozzle and with this configuration deposition rates of less than 10^{13} atom cm^{-2} s^{-1} were obtained over the entire sample. Low deposition rates were essential to produce samples with sufficiently small, well controlled coverages, to ensure only a fractional coverage of clusters at the steps on the surface. The deposition rate of neutral Ag atoms was measured by a quartz-crystal oscillator, located on a shutter directly in front of the substrates. The substrate size was 4 mm × 4 mm and up to three substrates could be mounted simultaneously on a

* Basis of the presentation given at Dalton Discussion No. 1, 3rd–5th January 1996, University of Southampton, UK.

Non-SI units employed: Torr ≈ 133 Pa, eV ≈ 1.60×10^{-19} J.

rotatable substrate holder, for separate depositions. The samples could be heated and their temperature monitored using a K-type thermocouple. Deposition times varied from 5 to 20 s over which period the deposition rate remained constant. The samples were then transferred in air and examined either by SEM (Hitachi S900) or bench-top STM (Burleigh or Nanoscope II). All the STM images presented here were taken in the constant-current mode with currents between 1 and 2 nA and sample biases between 2 and 330 mV. Platinum–iridium STM tips were prepared by etching with a sodium cyanide solution.

Cluster beam deposition

The cluster beam source used in these experiments is based on the inert-gas condensation principle.[15–17] Briefly, Ag is evaporated from a heated crucible inside a condensation chamber. The metal vapour is cooled by a flowing stream of helium gas at room temperature and a pressure of about 3–4 Torr, which causes condensation of the metal vapour into clusters with sizes ranging from a few atoms up to about a few hundred atoms. As the Ag–He mixture flows out of the condensation chamber it undergoes a weak supersonic expansion[18] into a region at a pressure of about 10^{-4} Torr (pumped by a 3000 l s^{-1} diffusion pump). A hot-cathode, magnetically confined plasma ionises the emerging cluster beam,[19] after which it passes through a skimmer into a second chamber which contains a Wien filter and the substrate. This chamber is pumped by a diffusion pump fitted with a water-cooled baffle. The pumping speed above the baffle is 1300 l s^{-1}, which results in a base pressure of 10^{-7} Torr and a partial pressure of He of less than 10^{-5} Torr during deposition at the position of the sample. The Wien filter (Colutron velocity filter, model 600-B)[20] allows mass selection of the beam prior to deposition, although in the experiments described here the Wien filter was run with only moderate mass resolution. The impact energy of the clusters on the graphite substrate was varied in the range 50–400 eV simply by adjusting the potential applied to the substrate, the ion source being kept at a fixed potential. All the samples were deposited at room temperature and were transferred in air to a Hitachi S900 scanning electron microscope for analysis.

Results and Discussion

Atomic vapour deposition

Nucleation of clusters at steps. Fig. 1(*a*) is a SEM image showing silver clusters on the surface of graphite following atomic vapour deposition at room temperature. The cluster density on the steps is significantly higher than that on the terrace, indicating that the clusters have grown preferentially along the steps. Clusters have also nucleated on the wider terraces, but not on the narrower ones. This is because the atoms landing on the narrower terraces can reach a step and be captured before colliding with another atom on the terrace. Thus, terrace nucleation is suppressed on the narrow terraces. On the wider terraces, however, some of the atoms can collide with each other before reaching a step, resulting in cluster growth on the terrace itself. With increasing temperature and thus an increasing hopping rate of the atoms on the terrace, all of the deposited Ag atoms can reach the steps. This results in the nucleation of clusters exclusively at the steps with empty terraces inbetween, as seen in Fig. 1(*b*). From Fig. 1(*a*) it can also be seen that the clusters produced on the terraces have formed into small groups, and therefore that the clusters (diameter ≈ 10 nm) must be mobile over short distances. For a given deposition rate and temperature, the linear density of clusters nucleated on a step should depend only on the terrace area adjacent to the step available for the collection of adatoms

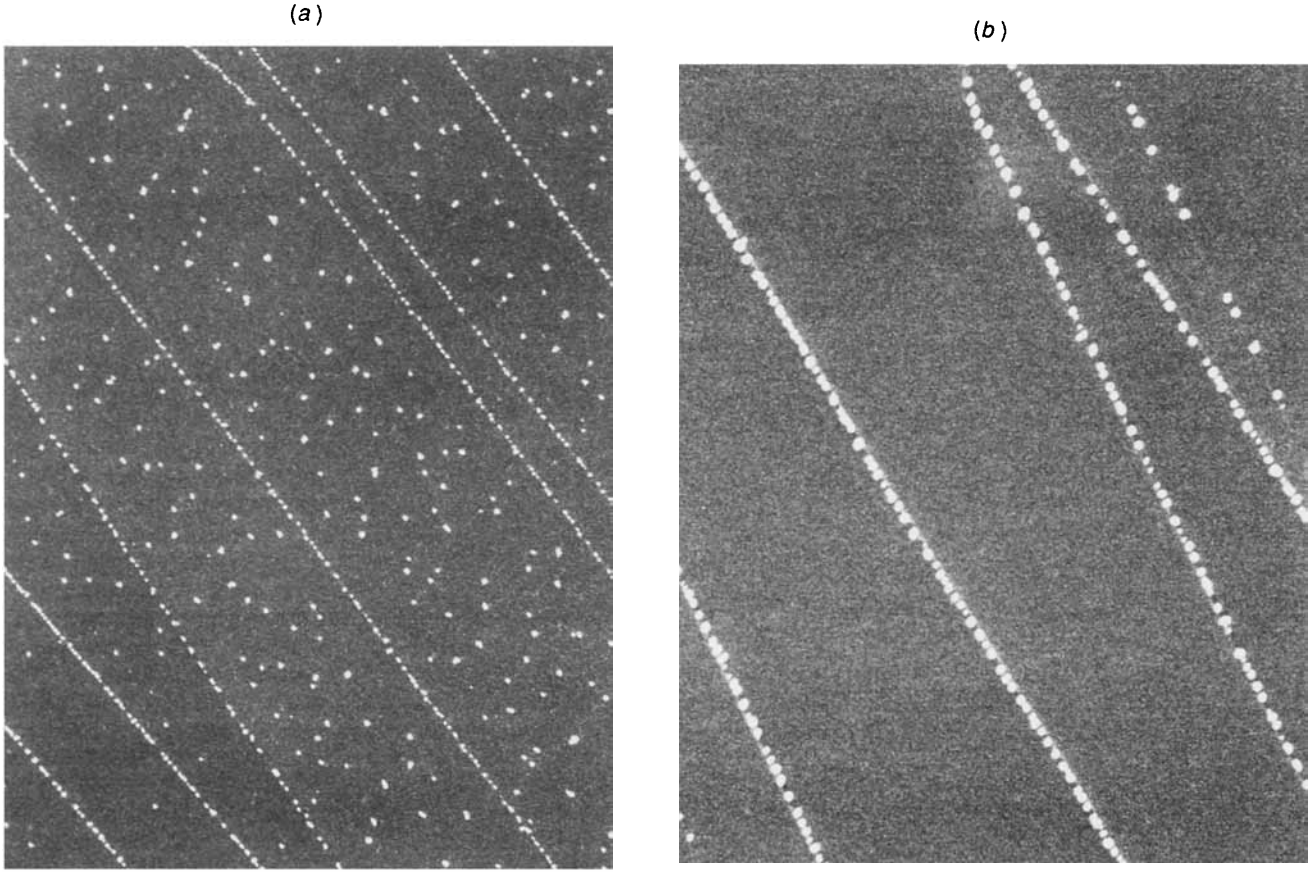

Fig. 1 The SEM images (*a*) (2.89 × 3.88 μm) of HOPG after deposition of 0.029 monolayer of Ag over 2 s at 20 °C, showing clusters on surface steps and terraces, (*b*) (1.23 × 1.67 μm) of HOPG after deposition of 0.046 monolayer of Ag over 3 s at 165 °C, showing clusters on surface steps only

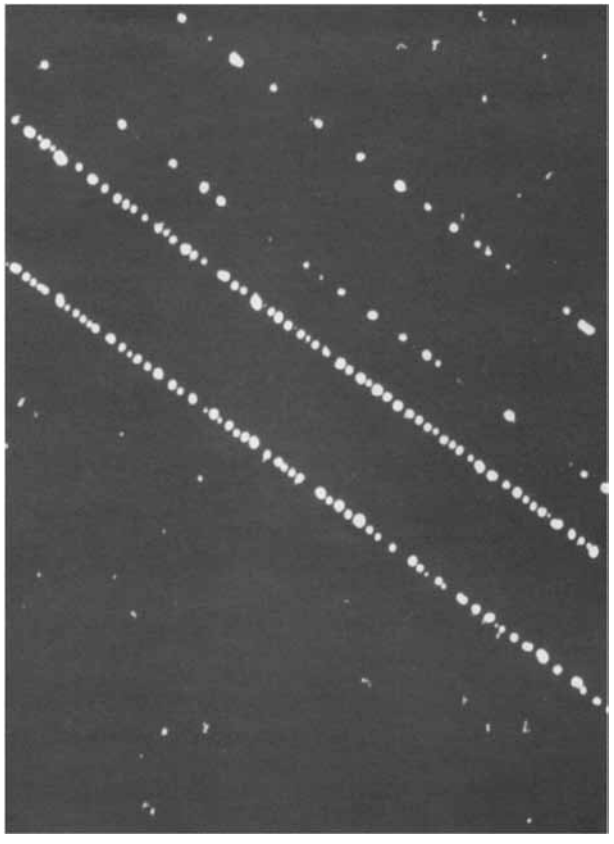

Fig. 2 A SEM image (1.45 × 1.94 μm) of HOPG after deposition of 0.075 monolayer of Ag over 2 s at 120 °C, showing different densities of silver clusters on steps (two central steps) with similar size collection widths

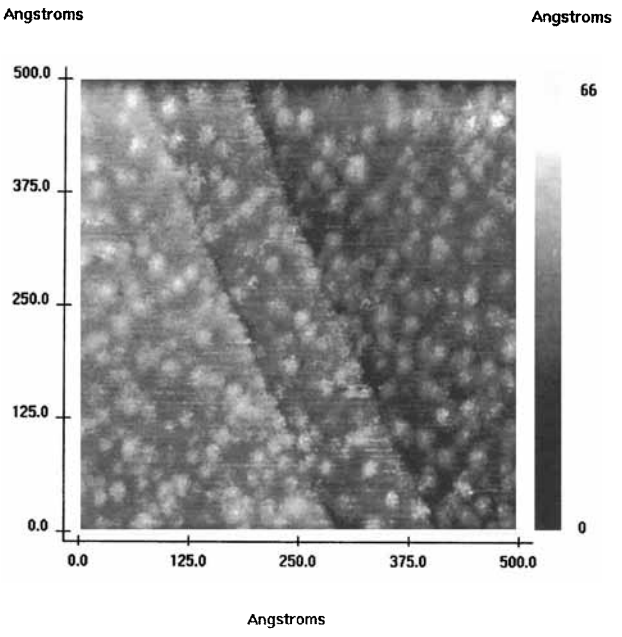

Fig. 3 A STM image (500 × 500 Å) of HOPG after deposition of 0.36 monolayer of Au over 10 s at 20 °C, showing two steps without clusters attached to them. The left one is one atomic layer high, the right three atomic layers high. Tunnelling current I = 0.9 nA, sample bias = +330 mV

(the 'collection width' of the steps), and the hopping rate along the steps. However, we have noticed that some steps with a similar collection width nucleate surprisingly different numbers of clusters: see Fig. 2 for an example; the two middle steps have nucleated vastly different numbers of clusters even though their collection widths are almost the same. A possible difference between these parallel steps is their respective heights. In order further to understand the interaction of adatoms and clusters with the surface we thus began an STM study of this system.

According to Ganz *et al.*,[4] Ag and Au atoms deposited on the surface of graphite behave similarly. They were both seen to produce two-dimensional islands, weakly bonded and incommensurate with the substrate. We have therefore investigated the deposition of both Ag and Au adatoms on the surface. Fig. 3 shows a high coverage (0.36 monolayer) of Au on the surface. The image shows two steps on the surface; to the left is a step one atomic layer high, and to the right a step three atomic layers high. Neither of these steps appears to be preferentially decorated with clusters. We have also seen similar results in the case of silver deposition. From this we can surmise that these shallow steps do not sufficiently trap the Ag and Au adatoms on the surface for nucleation to occur at room temperature. The adatoms seem to have enough energy to diffuse over the steps (or be reflected from them) without becoming adsorbed; thus it would appear that the steps which were decorated with clusters in our earlier SEM study must have been larger than three atomic layers high. So the capacity for a step to capture an adatom, *i.e.* to act as a perfect adatom 'sink' and then nucleate a cluster, seems to increase with step height.

Fig. 4(*a*) shows a STM topograph (1000 × 1000 Å) showing an array of clusters with an average size of 2 nm and also a flake of graphite about 30 nm long. Fig. 4(*b*) shows the same area of the substrate (except for a slight drift in the image) 5 min later, after ten consecutive STM scans. We observed that the STM tip disturbed and damaged the flake of graphite on the surface, ultimately fragmenting it. However, it was established that the clusters did not move over the 5 min period. We therefore conclude that the scanning of the tip does not affect the position of the clusters. Hence, it is not probable that the tip would move clusters away from steps, where the clusters are expected to bond more strongly than on the terrace. The absence of clusters at steps with small height (Fig. 3) cannot therefore be explained by tip-induced displacement of clusters.

Another conclusion which follows from Fig. 4 is that clusters of diameter ≈2 nm are stable with respect to diffusion on the terrace on the time-scale of minutes. This contrasts with the behaviour of larger clusters, ≈10 nm, which appear to diffuse and aggregate into larger island structures, as noted above, and suggests a complex, size-dependent mobility.

Clusters on terraces. We have also analysed two- and three-dimensional silver clusters on the substrate with STM. Fig. 5 shows a two-dimensional island of Ag made up of about 12 atoms with a diameter of approximately 1.5 nm and height ≈1.6 Å. The surrounding substrate has the hexagonal structure expected on graphite and most of the cluster atoms appear to align with the B sites, which show up as bright dots on the HOPG surface. This was found to be typical for all similarly sized islands imaged on the surface. We believe that the cluster–surface interaction may be responsible for the limited mobility of the smaller clusters discussed above.

Fig. 6 shows three two-dimensional clusters, and in each case the presence of the clusters has caused an enhancement of the surface charge density of the graphite around them. In fact it is difficult to determine exactly how large these clusters are, due to this enhancement of the charge density. By looking at a lower-contrast image, approximately 12 adatoms can be seen to protrude from the surface in the larger cluster. The charge-density enhancement decays over a distance of about 10 Å from the island, as seen with other metals, *e.g.* Mo.[8] A possible explanation for the enhancement of the surface charge density is that we are observing the screening charge which surrounds a cluster with partial ionic character. This effect has been modelled by Ishida and Palmer[21] for the case of potassium

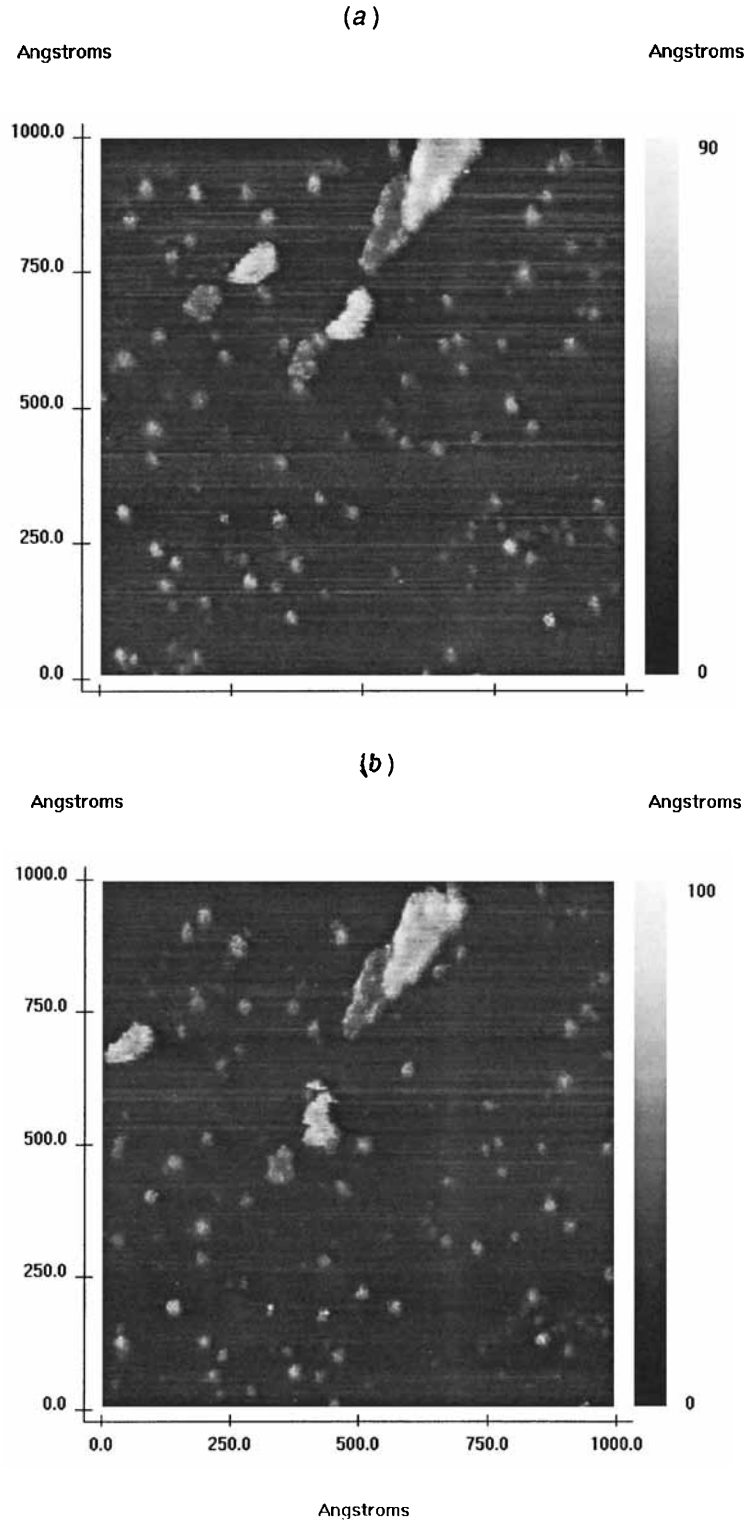

Fig. 4 The STM images (1000 × 1000 Å) of HOPG (*a*) after deposition of 0.09 monolayer of Ag over 15 s at 20 °C, showing 2 nm silver clusters and a graphite flake (tunnelling current I = 1.9 nA, sample bias = +110 mV), (*b*) as (*a*) viewed 10 scans and 5 min later

atom adsorption on HOPG. These authors found that, compared with a metal, the screening charge in graphite is quite delocalised due to its semimetallic band structure.

Fig. 7(*a*) shows a three-dimensional cluster, with a diameter of 3 ± 0.2 nm and a height of about 0.34 nm, which corresponds to the height of approximately two atomic layers of Ag. Charge-density modulations can be seen clearly above and below this cluster. Fig. 7(*b*) shows the CDM above this cluster more clearly. It has a periodicity consistent with a ($\sqrt{3} \times \sqrt{3}$)-rotated 30° modulation, just like the periodicities reported in the case of other adsorbed particles on graphite. On the lower right of the image the normal graphite structure can be seen; the angle between the rows of atoms in this region and the rows of the CDM can be seen to be close to 30°. Note that the surface appears artificially featureless to the centre left and right of the cluster in the tip scanning direction, because the tip was scanning too fast for it to compensate for the abrupt change in height. Interestingly we have not found any two-dimensional clusters giving rise to a CDM. In fact, Ganz *et al.*[4] looked at very large two-dimensional clusters of Ag and Au in detail and did not report any CDMs.

It seems that the origin of the CDM may lie in an interaction

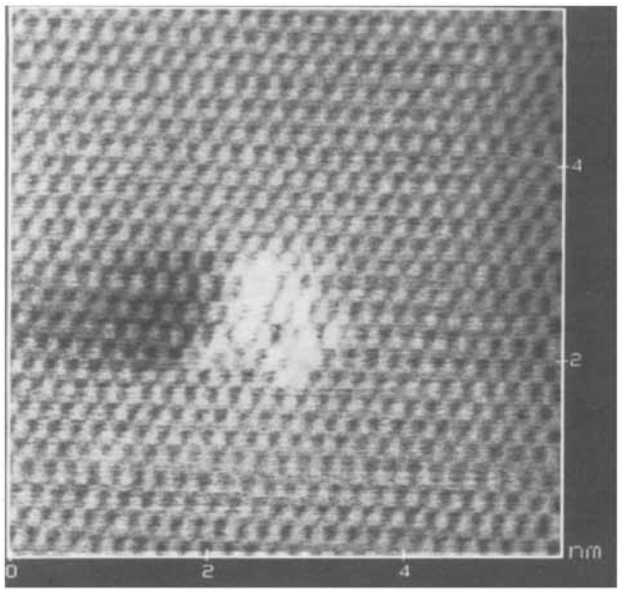

Fig. 5 A STM image (60 × 60 Å) of HOPG after deposition of 0.06 monolayer of Ag over 8 s at 20 °C, showing a two-dimensional island of Ag. Tunnelling current I = 1.8 nA, sample bias = +2.1 mV

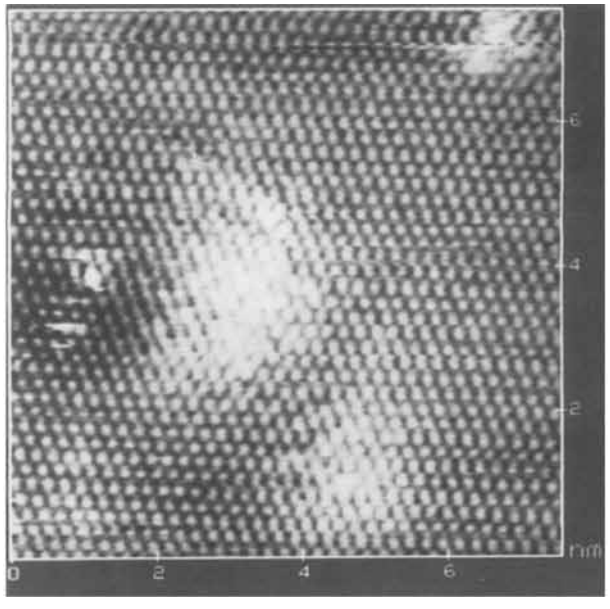

Fig. 6 A STM image (80 × 80 Å) of HOPG after deposition of Ag, showing three two-dimensional clusters with surface charge-density enhancement. Deposition conditions as in Fig. 5

between the d bands of the cluster and the Fermi level of the substrate. It has been shown for three-dimensional platinum (and palladium) clusters that the d bands broaden and approach the Fermi level as the size of the cluster increases[22] on a strongly interacting substrate, Ag(110). This is probably due to the increasing number of platinum (or palladium) neighbours. We speculate that a similar effect may also occur on graphite. It has also been noted that the decay length of the CDM produced by platinum clusters (up to 5 nm) is larger than that produced by palladium clusters (2 nm), and this has been attributed to the larger width of the d band in Pt compared with Pd.[23] Since the d band of Pd is wider than that of Ag, and closer to the Fermi level,[24] it would therefore be expected that the threshold size for silver clusters to produce CDMs will be larger than for Pd. Consistent with this, ref. 13 reports a CDM around a cluster with an average diameter of 2.2 ± 0.5 nm, while we have only seen CDMs around three-dimensional silver clusters larger than 3 ± 0.2 nm in diameter.

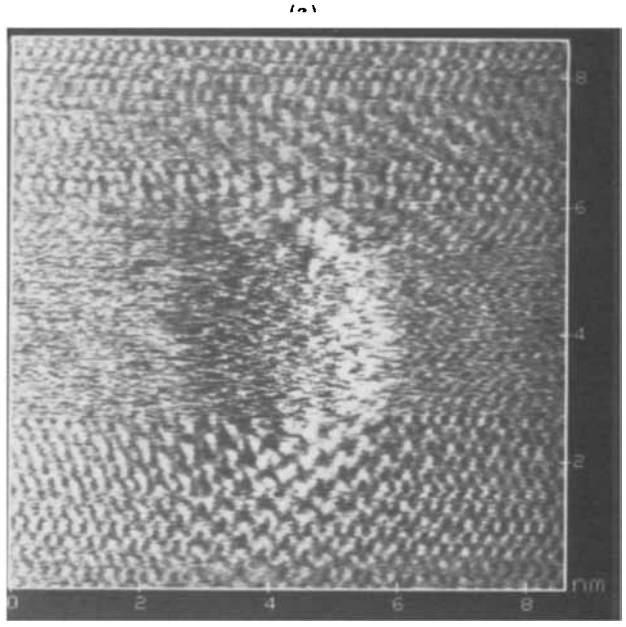

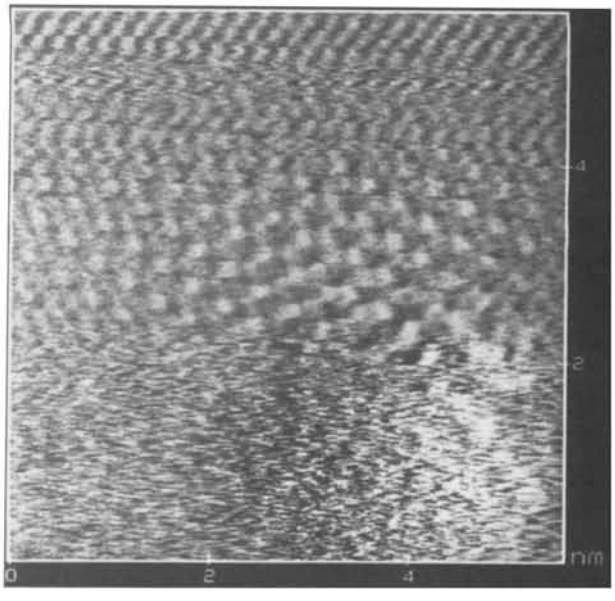

Fig. 7 The STM images (85 × 85 Å) of HOPG (*a*) after deposition of Ag, showing a three-dimensional cluster surrounded by charge-density modulations; the 30° angle between rows in the charge-density modulation area and the underlying lattice row direction is marked (deposition conditions as in Fig. 5); (*b*) the top part of (*a*) showing charge-density modulations

Fig. 8 shows a small two-dimensional cluster comparable in size to those seen in Fig. 5 but in this case it has produced a CDM. A defect can be seen in the surface as a dark spot surrounded by three atoms at the top of the cluster. We believe that this defect is the cause of the CDM (and in this case, probably also the cluster nucleation site), since two-dimensional clusters of similar size without defects do not form CDMs. The result also suggests a method of identifying a defect even when it may be obscured by a cluster, as long as the cluster does not produce a CDM of its own, *i.e.* it is small and two-dimensional. By using this identification procedure, we found that defect nucleation plays an insignificant role in the growth of clusters on the HOPG terrace, in fact only one example has been identified although many two-dimensional clusters have been examined in this study. Defect nucleation is a very important

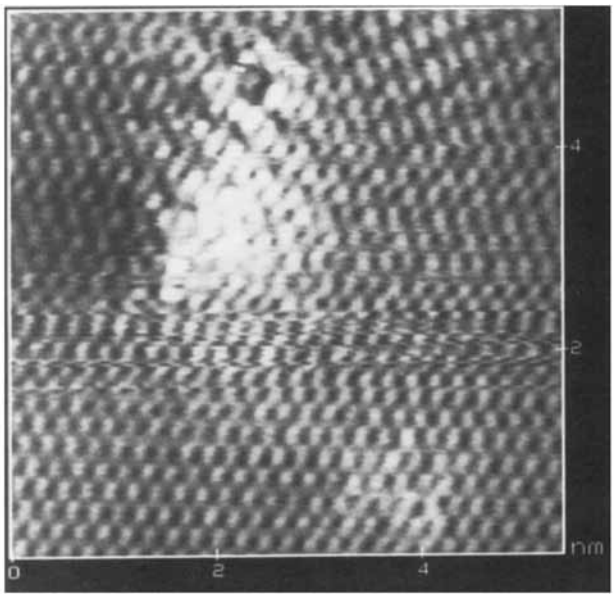

Fig. 8 A STM image (110 × 110 Å) of HOPG after deposition of Ag, showing a two-dimensional cluster nucleated around a defect. Deposition conditions as in Fig. 5

factor in some nucleation theories, for example, for Au on alkali-metal halide substrates.[25]

Cluster beam deposition

In the final part of this paper we present a brief account of new experiments exploring the deposition of silver clusters on HOPG from a cluster beam source, with a particular focus on the deposition dynamics as a function of the cluster–surface impact energy.

Fig. 9 displays two SEM micrographs, showing clusters deposited with impact energies of 50 and 400 eV respectively. In both cases the number of clusters deposited per unit surface area was 0.016 nm^{-2}, estimated from the total charge collected by the sample under the assumption of singly charged clusters. The mean cluster size in the incident beam was approximately 160 atoms. A marked difference between the two pictures can be observed. In the lower impact energy (50 eV) case, Fig. 9(*a*), fractal islands have developed on the graphite terraces, each fractal consisting of about ten particles; the average particle diameter is 9 nm. Similar particles are seen to decorate the step edge. Assuming that these particles are two-dimensional islands, one can deduce that approximately 10 deposited clusters have aggregated to form each particle *via* diffusion over the substrate. These observations demonstrate (*a*) that the deposited clusters are mobile on the surface, (*b*) that the particles produced by cluster aggregation are also mobile, and (*c*) that the cluster aggregation stops once a particle size of ≈ 10 nm is reached. We note also that the mean size of the particles decorating the step is 7 nm, *i.e.* smaller than those on the terrace, which suggests a reduced mobility of clusters along the steps.

Turning to the higher impact energy case (400 eV), Fig. 9(*b*), the picture is quite different. We find no evidence of decoration of the steps on the surface and the particles observed are much smaller corresponding (at least approximately) to the size of the incident clusters. Both these observations are evidence that the clusters are not mobile on the surface. Recent simulations[26] have shown that Cu_{147} clusters impacting onto the Cu(111) surface may cause various degrees of damage to the surface, depending on the energy. In particular, at 193 eV the clusters partially penetrate the surface leading to a certain amount of intermixing, while at 773 eV they penetrate deep into the surface leading to significant surface damage and crater formation. We thus expect that silver clusters impinging on graphite with

(*a*)

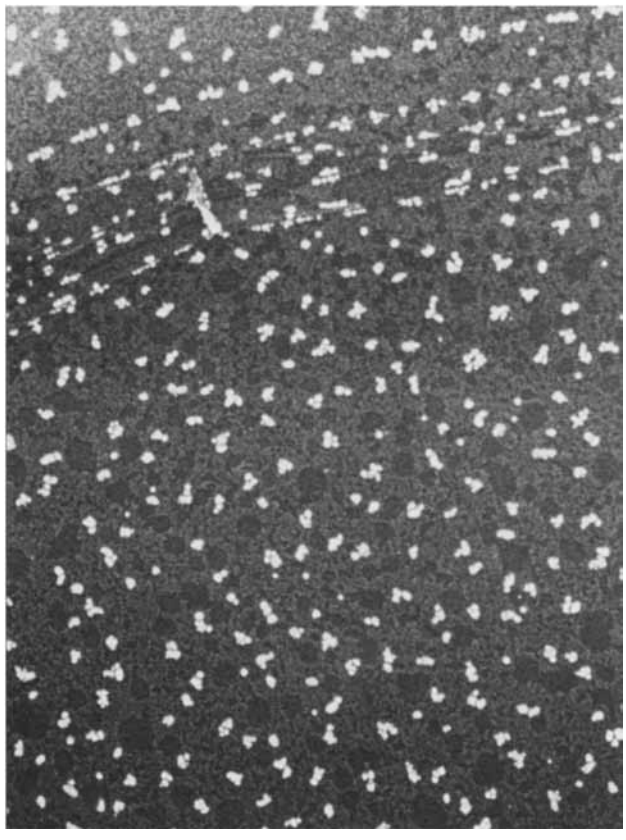

(*b*)

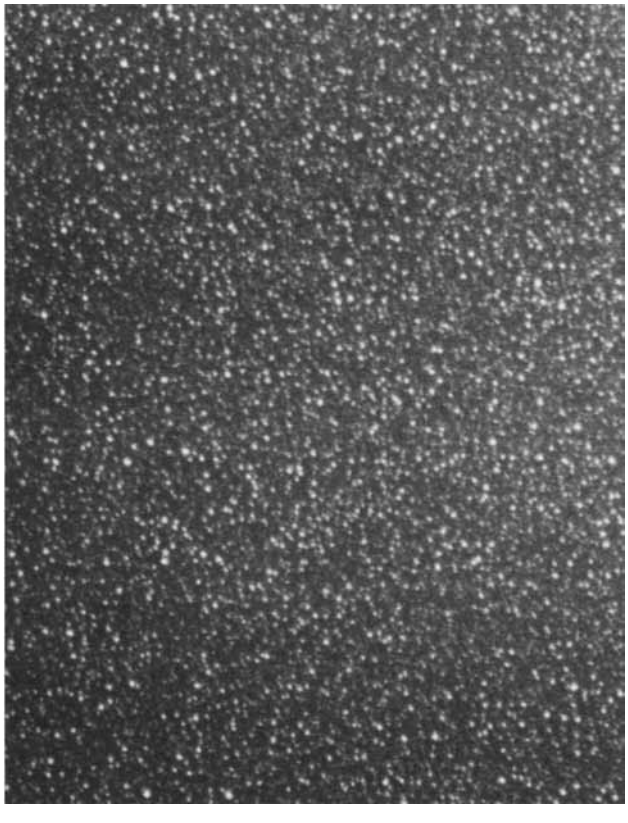

Fig. 9 The SEM images showing Ag_n^+ clusters (n = 20–300 atoms) deposited on HOPG at 20 °C, surface coverage 0.016 clusters nm^{-2}: (*a*) (1.3 × 0.97 μm) 50 eV impact energy, (*b*) (670 × 510 nm) 400 eV impact energy

400 eV of kinetic energy may also be implanted, preventing diffusion and aggregation. This is supported by the fact that the minimum energy necessary to create stable defects in HOPG by rare gas ions is 34.5 eV.[27]

Conclusions

We have studied the deposition and growth of silver and gold clusters on the surface of graphite. Two types of experiments were performed: evaporation of Ag or Au atoms onto the surface with subsequent STM and SEM examination, and deposition of Ag_n^+ clusters as a function of impact energy with subsequent SEM examination.

In the case of atomic vapour deposition on graphite we have shown that the interaction between the deposited atoms and surface steps depends on the step height. For shallow steps (one and three atomic layers in height) we have not observed preferential nucleation in comparison with growth on the terraces. On the terraces we have identified small (1–2 nm in diameter) immobile, two-dimensional clusters which are at least partly commensurate with the substrate and may be stabilised by ionic bonding. Larger (> 3 nm) three-dimensional clusters give rise to charge-density modulations in the surrounding substrate.

The results of ionised cluster-beam (Ag_n^+) deposition on graphite depend greatly on the cluster impact energy. For an impact energy of 400 eV we have found evidence for cluster implantation. At lower energies (*e.g.* 50 eV) diffusion and aggregation of the incident clusters has been observed. These new experiments demonstrate the possibility of controlling the growth of novel surface nanostructures *via* metal cluster deposition.

Acknowledgements

We thank the EPSRC and the Royal Society for financial support of this work. G. M. F. and I. M. G. acknowledge the EPSRC for the award of studentships. G. M. F. is grateful to Dr. N. Berovic for access to the Burleigh scanning tunelling microscope. L. Kuipers acknowledges financial support as a Human Capital and Mobility Research Fellow.

References

1 S. N. Khanna and P. Jena, *Phys. Rev. Lett.*, 1992, **69**, 1664.
2 W. Chen, H. Ahmed and K. Nakazato, *Appl. Phys. Lett.*, 1995, **66**, 3383.
3 G. M. Francis, L. Kuipers, J. R. A. Cleaver and R. E. Palmer, *J. Appl. Phys.*, in the press.
4 E. Ganz, K. Sattler and J. Clarke, *Phys. Rev. Lett.*, 1988, **60**, 1856.
5 J. Xhie, K. Sattler, U. Müller, N. Venkateswaran and G. Raina, *Phys. Rev. B*, 1991, **43**, 8917.
6 J. Valenzuela-Benavides and L. Morales de la Garza, *Surf. Sci.*, 1995, **330**, 227.
7 F. J. Cadete Santos Aires, P. Sautet and J.-L. Rousset, *J. Vac. Sci. Technol. B*, 1994, **12**, 1776.
8 H. Xu, H. Permana, Y. Lu and K. Y. S. Ng, *Surf. Sci.*, 1995, **325**, 285.
9 J. Yan, Z. Li, C. Bai, W. S. Yang, Y. Wang, W. Zhao, Y. Kang, F. C. Yu, P. Zhai and X. Tang, *J. Appl. Phys.*, 1994, **75**, 1390.
10 T. R. Albrecht, H. A. Mizes, J. Nogami, Sang-il Park and C. F. Quate, *Appl. Phys. Lett.*, 1988, **52**, 362.
11 H. A. Mizes and J. S. Foster, *Science*, 1989, **244**, 559.
12 J. Valenzuela, L. Morales de la Garza, M. Avalos-Borja and S. Fuentes, *J. Phys.: Condensed Matter*, 1993, **5**, A413.
13 F. J. Cadete Santos Aires, P. Sautet, G. Fuchs, J.-L. Rousset and P. Mélinon, *Microsc. Microanal. Microstruct.*, 1993, **4**, 441.
14 E. Ganz, K. Sattler and J. Clarke, *Surf. Sci.*, 1989, **219**, 33.
15 D. M. Mann and H. P. Broida, *J. Appl. Phys.*, 1973, **44**, 4950.
16 A. Yokozeki and G. D. Stein, *J. Appl. Phys.*, 1978, **49**, 2224.
17 W. A. de Heer, *Rev. Mod. Phys.*, 1993, **65**, 611.
18 R. Miller, in *Atomic and Molecular Beam Methods*, ed. G. Scoles, Oxford University Press, 1988, vol. 1, ch. 2, p. 50.
19 K. M. McHugh, H. W. Sarkas, J. G. Eaton, C. R. Westgate and K. H. Bowen, *Z. Phys. D*, 1989, **12**, 3.
20 L. Wahlin, *Nucl. Instrum. Methods*, 1964, **27**, 55.
21 H. Ishida and R. E. Palmer, *Phys. Rev. B*, 1992, **46**, 15 484.
22 H. V. Roy, P. Fayet, F. Patthey, W. D. Schneider, B. Delley and C. Massobrio, *Phys. Rev. B*, 1994, **49**, 5611; H. V. Roy, J. Boschung, P. Fayet, F. Patthey and W. D. Schneider, *Z. Phys. D*, 1993, **26**, 252.
23 P. Sautet and J. F. Paul, *Catalysis Lett.*, 1991, **9**, 245.
24 T. K. Sham, *Phys. Rev. B*, 1985, **31**, 1888.
25 A. D. Gates and J. L. Robins, *Thin Solid Films*, 1987, **149**, 113.
26 H.-P. Cheng and U. Landman, *J. Phys. Chem.*, 1994, **98**, 3527.
27 D. Martin, H. Bu, K. J. Boyd, S. S. Todorov, A. H. Al-Bayati and J. W. Rabalais, *Surf. Sci.*, 1995, **326**, L489.

Received 18*th September* 1995; *Paper* 5/06745F